A procedure for the static analysis of cable structures following elastic catenary theory

Leopoldo Greco, Nicola Impollonia, Massimo Cuomo

A procedure for the static analysis of cable structures following elastic catenary theory

L. Greco, N. Impollonia *, M. Cuomo

Dipartimento di Ingegneria Civile ed Ambientale (DICA), Universitá degli Studi di Catania, V.le A. Doria 6, 95100 Catania, Italy

A B S T R A C T

The paper proposes an unitary strategy for the static analysis of general cable nets under conservative loads. A form-finding is first performed in order to initialize the successive non linear analysis. The numerical procedures carried on in both steps, form finding and structural analysis of the net, employ a three dimensional elastic catenary element. Equilibrium conditions at internal nodes and kinematic compatibility at the end nodes of each cable are used to derive the global equations of the net. When the pre-stresses are high and the topology of the net is involved, an accurate initializing solution is essential for the convergence of the successive numeric non linear structural analysis (performed by Newton method). The numerical applications highlight the capability of the proposed procedure to solve three dimensional problems with taut and slack cables, out of plane distributed forces (modeling wind loads), point loads along the cables. The contemporary presence of cables and compression truss elements is also considered testing the effectiveness of the method in the analysis of tensegrity structures.

1. Introduction

An effective and accurate cable model is a main requisite for the analysis of cable structures. A most desirable property is the capability to perform well for both the case of taut and sagged cables. Furthermore, accuracy and presence of point forces along the cables should not rely on sub-element division. In this way the nodes are located at cable intersections and external points only. Such requisites can only be met by catenary elements, first introduced by Peyrot and Goulois (1978, 1979) and Jayaraman and Knudson (1981) and extended to the case of non-conservative constant load in Ahmadi-Kashani and Bell (1986, 1988a,b). Catenary elements without internal joints have been implemented to solve real engineering problems and have been proven to perform better than finite elements based on interpolation functions (Irvine, 1992). The study reported in Freire et al. (2006) highlights that pseudo linear approaches and modified modulus elements are inappropriate to analyze steel cable-stayed bridges as the non linear effects produced by the coupling between cable sag and large displacements, a decisive issue in the global behavior of those structures, can be accurately estimated by catenary elements. The strong nonlinearities arising in cable-pulley systems such as ski lifts, electrical transmission lines and long-span bridges are correctly reproduced following the catenary model (Bruno and Leonardi, 1999; Such et al., 2009), which is also suitable for dynamic analysis (Thai and Kim, 2011) and cable damage evaluation (Lepidi et al., 2007). However, in the study of dynamics and stability of shallow cables, an asymptotic analytical model is commonly used in which the catenary is well approximated by a parabola, see Lee and Perkins (1992) and Luongo and Piccardo (1998, 2008), the actual influence of this hypothesis could be verified by using a numerical procedure based on elastic catenary elements.

The catenary cable element can take into account elastic deformation and, when the three dimensional analytical equations are formulated in the global reference system, it allows a simpler resolution of cable nets (Andreu et al., 2006). Closed form solution have also been presented to encompass concentrate and distributed forces along the cable without increasing the number of nodes (Sagatun, 2001; Impollonia et al., 2011).

Although the advantage of using cable elements based on catenary solution has been established in the literature, their capability to tackle more complex layout with several nodes and general loads has not been fully investigated and it will be the goal of the present paper. To this aim the initial state under cable prestresses and cable self weight must be accurately predicted by a suitable form finding procedure. This solution will be the initializing step for the subsequent analysis with additional external loads occurring during life service such as wind loads, snow loads and cladding. Different approaches to the form finding problem of self-stressed structures are available in the literature, i.e. *force*

* Corresponding author. Tel.: +39 0931489425.

E-mail addresses: leopoldo.greco@virgilio.it (L. Greco), nimpo@unict.it (N. Impollonia), mcuomo@unict.it (M. Cuomo).

density method (FDM), *dynamic relaxation* and *natural strain*. In this work we approach the form-finding by FDM. The concept of the force density as shape parameter was developed by Schek (1974). Successively Haber and Abel (1982) proposed the *assumed geometric stiffness method*, in which the force density parameter was given mechanical interpretation of geometric stiffness. On this research line Bletzinger and Ramm (1999) proposed the *up-dated reference strategy* as an iterative optimization procedure to detect the minimal surface. Analogously, Pauletti and Pimenta (2008) starting from the work of Argyris et al. (1974) presented a procedure called *natural force density method*.

Force densities play the role of degrees of freedom of the equilibrium shape which is singled out by a linear procedure or by a non linear one if some constraint are imposed with the aim to satisfy additional conditions. Deng et al. (2005) proposed a self weight parabolic element for the form-finding of slack cable nets in the analysis of the different configurations during the erection process of a cable net structure. Cuomo and Greco (2012) developed the *catenary force density method* (C-FDM), i.e. an extension of FDM including self weight of the catenary element in the form-finding.

The procedure proposed herein takes advantage of the non linear form-finding method developed in Cuomo and Greco (2012) which rigorously takes into account cable self weight in the equilibrium of the pre-stress state and that, therefore, can also be applied to slack cables or very heavy elements. In this case, indeed, the initial configuration determined with the equivalent truss element can be very far from the effective catenary configuration. This goal is reached retaining the exact equilibrium equations of the heavy cable. It is shown that the use of the exact equilibrium conditions leads to a form-finding method that is very similar to the standard force density method, although it requires the solution of a non linear system of equations. In this way an accurate initial configuration is produced for complex cable nets with both slack and taut cables.

Cable equations are derived in 3D vector form following (Impollonia et al., 2011), allowing cable elastic deformation, arbitrarily oriented constant distributed loads and in-span point forces. These equations specify, in closed form and with reference to the strained configuration: (i) the relationship, in the global reference system, between cable tension at the generic cable point and the same quantity at cable origin; (ii) the position of the generic cable point with reference to cable origin. The conditions of equilibrium at each internal node and kinematic compatibility at the end node of each cable are imposed according to cable connectivity so to derive the non linear global equations of the entire net. No recourse to rotation matrix is needed as the same reference system is adopted for all cables.

Numerical applications assess that the solution of the nonlinear system, with unknowns given by free nodes position and tension vector at cable origins, is easily determined by Newton method if unknown quantities are set to the initial values resulting from the preliminary form-finding. In this case even with slackening and decreasing of stiffness of some cables, the solution can be reached with few iterations (Impollonia et al., 2011).

Finally, the study of the Jawerth net (Mollmann, 1970) is carried on also with the aim to make a comparison of the results with those of other authors. A 3D version of the net, obtained by adding out of plane stay cables, is analyzed under the action of wind load modeled as a simple constant horizontal load on each cable. More refined wind load such as those presented in Lazzari et al. (2001), Di Paola (1998), Impollonia et al. (2011a,b) could be only be considered by adopting associate catenary formulations (Ahmadi-Kashani and Bell, 1988a).

2. Cable element formulation

The equilibrium equation is derived with reference to the internal tension of the cable, $\boldsymbol{\tau}(S)$, tangent to the current centroid curve (i.e. the cable in the strained configuration). The Lagrangian coordinate S, ($0 \leqslant S \leqslant L$ with L the length of the unstrained cable), represents the arc length of the unstrained cable between the generic centroid point and the cable origin. Indicating as $\mathbf{p} = \mathbf{p}(S)$ the position vector of the cable axis of the generic (strained) configuration, its tangent (non unit) vector can be written as $\mathbf{t} = \frac{d\mathbf{p}}{dS}$, then the unit tangent vector is given by $\hat{\mathbf{t}} = \frac{\mathbf{t}}{\|\mathbf{t}\|}$.

Linear elastic behavior, $\|\boldsymbol{\tau}\| = EA\varepsilon$, is considered where E is the Young's modulus and A is the cross-sectional area in the unstrained configuration; only small deformations are allowed so that $\varepsilon(S) = \frac{ds}{dS} - 1 > 0$ is the strain of the cable (s is the arc-length in the strained configuration).

2.1. The equilibrium equation

Let be $\mathbf{q}_S$ the distributed line load (referred to the unstrained configuration) acting on the cable, $\mathbf{R}^0$ and $\mathbf{R}^L$ the boundary forces at its ends. The equilibrium equations is cast as follows

$$-\frac{d\boldsymbol{\tau}}{dS} = \mathbf{q}_S, \tag{1}$$

so that at the boundaries

$$\boldsymbol{\tau}^0 = \boldsymbol{\tau}(0) = -\mathbf{R}^0, \quad \boldsymbol{\tau}^L = \boldsymbol{\tau}(L) = \mathbf{R}^L. \tag{2}$$

By integrating Eq. (1) in $[0, S]$, one gets

$$\boldsymbol{\tau}(S) = \boldsymbol{\tau}^0 - \int_0^S \mathbf{q}_S \, dS. \tag{3}$$

In the following, let us assume $\mathbf{q}_S$ to be constant over S, so that $\mathbf{q}_S(S) = \mathbf{q}_S = q_S\boldsymbol{\pi}$, where $q_S = \|\mathbf{q}_S\|$ is the intensity and $\boldsymbol{\pi}$ is the direction of the line load, both constant with S. Accordingly, Eq. (3) gives

$$\boldsymbol{\tau}(S) = \boldsymbol{\tau}^0 - \mathbf{q}_S S, \tag{4}$$

for the generic segment $[0, S]$ and globally

$$\boldsymbol{\tau}^L = \boldsymbol{\tau}^0 - \mathbf{q}_S L. \tag{5}$$

A graphic representation of the equilibrium equations (4) and (5) is shown in Fig. 1. Eq. (4) is suitable for cables under self weight, where $\mathbf{q}_S$ is the self weight per unit unstrained length. However, in practical applications of cable nets where the displacement produced by the external loads are small due to high initial pre-stress,

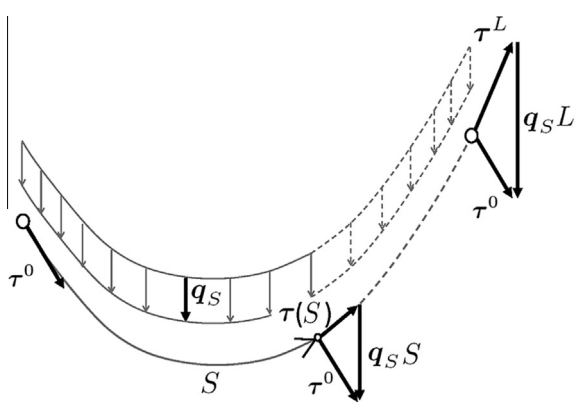

Fig. 1. Sketch of cable equilibrium; $\boldsymbol{\tau}^0, \boldsymbol{\tau}(S)$ and $\boldsymbol{\tau}^L$ are the internal tension at cable origin, generic abscissa S and cable end, respectively.

$\mathbf{q}_S$ can also model wind loads. More general cases, such as those related to the associate catenary cannot be correctly described by Eq. (4) and are discussed in Ahmadi-Kashani and Bell (1988a). In the following the pedex S will be omitted and the load q is tacitely referred to the unstrained configuration.

2.2. Elastic catenary solution

The equation governing the strained cable configuration is derived assuming uniform distributed load and also allowing the presence of an additional in-span point force.

2.2.1. Uniform distributed load

The equations of the equilibrated configuration of an extensible cable are derived under the assumptions of perfect shear and bending flexibility, following Impollonia et al. (2011). The case of a uniform distributed load, $\mathbf{q} = q\boldsymbol{\pi}$, is first considered.

The equilibrium equation for a segment $[0, S]$, with $S \leqslant L$, is given by (4) where $\boldsymbol{\tau}^0 = \{\tau_x^0, \tau_y^0, \tau_z^0\}$ is the vector collecting the tension force components at cable origin. Recalling that the cable tension is a vector along the current tangent of the cable configuration, one has

$$\hat{\mathbf{t}}(S) = \frac{\boldsymbol{\tau}(S)}{\|\boldsymbol{\tau}(S)\|}, \tag{6}$$

where, in virtue Eq. (4), the modulus of the tension is given by:

$$\|\boldsymbol{\tau}(S)\| = \|\boldsymbol{\tau}^0 - \mathbf{q}S\|. \tag{7}$$

It is not trivial to observe that this definition (as clear from Eq. (6)) rules out compression for the cable. Furthermore, assuming linear elastic behavior and small deformation one gets

$$\frac{ds}{dS} = \|\mathbf{t}\| = 1 + \varepsilon = 1 + \frac{\|\boldsymbol{\tau}(S)\|}{EA}. \tag{8}$$

Therefore, from Eqs. (6) and (8) the tangent vector splits in the sum of two addend

$$\mathbf{t} = \frac{d\mathbf{p}}{dS} = \|\mathbf{t}\|\hat{\mathbf{t}} = \left(1 + \frac{\|\boldsymbol{\tau}(S)\|}{EA}\right)\frac{\boldsymbol{\tau}(S)}{\|\boldsymbol{\tau}(S)\|} = \frac{\boldsymbol{\tau}(S)}{\|\boldsymbol{\tau}(S)\|} + \frac{\boldsymbol{\tau}(S)}{EA}. \tag{9}$$

The sought closed form of catenary equation,

$$\mathbf{p}(S) = \mathbf{p}(0) + \int_0^S \mathbf{t}\,dS, \tag{10}$$

is obtained exploiting Eq. (9) and can be cast in the following form:

$$\mathbf{p}(S) = \mathbf{p}(0) + \mathbf{p}_c(S) + \mathbf{p}_\varepsilon(S), \tag{11}$$

with

$$\mathbf{p}_c(S) = \int_0^S \frac{\boldsymbol{\tau}(S)}{\|\boldsymbol{\tau}(S)\|}dS, \quad \mathbf{p}_\varepsilon(S) = \frac{1}{EA}\int_0^S \boldsymbol{\tau}(S)dS, \tag{12}$$

where $\mathbf{p}(0)$ is cable origin position, $\mathbf{p}_c(S)$ represents the unstrained solution while $\mathbf{p}_\varepsilon(S)$ gives the contribute of the elastic increment. The second integral can be easily solved, so to give:

$$\mathbf{p}_\varepsilon(S) = \frac{qS}{EA}\left(\frac{\boldsymbol{\tau}^0}{q} - \boldsymbol{\pi}\frac{S}{2}\right). \tag{13}$$

The first integral in Eq. (12) requires some manipulations that are exposed in Impollonia et al. (2011) and can be written as follows:

$$\mathbf{p}_c(S) = (\mathbf{I} - \boldsymbol{\pi}\boldsymbol{\pi}^T)\frac{\boldsymbol{\tau}^0}{q}\ln\left[\frac{\rho(S)}{\rho(0)}\right] - \boldsymbol{\pi}\left(\left\|\frac{\boldsymbol{\tau}^0}{q} - \boldsymbol{\pi}S\right\| - \left\|\frac{\boldsymbol{\tau}^0}{q}\right\|\right), \tag{14}$$

where the function $\rho(S)$ is defined as:

$$\rho(S) = \|\boldsymbol{\tau}(S)\| - \boldsymbol{\pi}^T\boldsymbol{\tau}(S) = \|\boldsymbol{\tau}^0 - \mathbf{q}S\| - \boldsymbol{\pi}^T(\boldsymbol{\tau}^0 - \mathbf{q}S). \tag{15}$$

Finally, the strained configuration of the cable is given by

$$\mathbf{p}(S) = \frac{qS}{EA}\left(\frac{\boldsymbol{\tau}^0}{q} - \boldsymbol{\pi}\frac{S}{2}\right) + (\mathbf{I} - \boldsymbol{\pi}\boldsymbol{\pi}^T)\frac{\boldsymbol{\tau}^0}{q}\ln\left[\frac{\rho(S)}{\rho(0)}\right] - \boldsymbol{\pi}\left(\left\|\frac{\boldsymbol{\tau}^0}{q} - \boldsymbol{\pi}S\right\| - \left\|\frac{\boldsymbol{\tau}^0}{q}\right\|\right) + \mathbf{p}(0). \tag{16}$$

Once $\boldsymbol{\tau}^0$ and $\mathbf{p}(0)$ are determined, the length of a strained segment of the cable can be evaluated by means of Eq. (8):

$$s(S) = \int_0^S \left(1 + \frac{\tau(S)}{EA}\right)dS = S + \Delta L(S), \tag{17}$$

with the global elongation

$$\Delta L = \int_0^L \frac{\tau(S)}{EA}\,dS \tag{18}$$

and strained length of the cable $l = L + \Delta L$. Fig. 2 sketches the defined quantities.

2.2.2. Additional one point force

Let us assume that one point force $\mathbf{f}$ is applied at abscissa $\bar{S}$ on the cable along with the distributed load $\mathbf{q}$. The equilibrium equation of the generic cable segment, analogous to (4), in this case is given by

$$\boldsymbol{\tau}(S) = \boldsymbol{\tau}^0 - \mathbf{f}\mathrm{U}[S - \bar{S}] - \mathbf{q}S, \tag{19}$$

where $\mathrm{U}[S - \bar{S}]$ is the unit step function. For $S \leqslant \bar{S}$ the equilibrium solution reduces to that for cables with distributed load only, Eq. (16), while for $S > \bar{S}$, see Impollonia et al. (2011), the solution is given by

$$\begin{aligned}\mathbf{p}(S) = {} & \frac{q}{EA}\left(\frac{\boldsymbol{\tau}^0 S}{q} - \frac{\mathbf{f}(S - \bar{S})}{q} - \frac{\boldsymbol{\pi}S^2}{2}\right) + (\mathbf{I} \\ & - \boldsymbol{\pi}\boldsymbol{\pi}^T)\left(\frac{\boldsymbol{\tau}^0}{q}\ln\left[\frac{\rho(\bar{S})\rho_F(S)}{\rho(0)\rho_F(\bar{S})}\right] - \frac{\mathbf{f}}{q}\ln\left[\frac{\rho_F(S)}{\rho_F(\bar{S})}\right]\right) \\ & - \boldsymbol{\pi}\left(\left\|\frac{\boldsymbol{\tau}^0}{q} - \frac{\mathbf{f}}{q} - \boldsymbol{\pi}S\right\| + \left\|\frac{\boldsymbol{\tau}^0}{q} - \boldsymbol{\pi}\bar{S}\right\| - \left\|\frac{\boldsymbol{\tau}^0}{q}\right\| - \left\|\frac{\boldsymbol{\tau}^0}{q} - \frac{\mathbf{f}}{q} - \boldsymbol{\pi}\bar{S}\right\|\right) \\ & + \mathbf{p}(0),\end{aligned} \tag{20}$$

with

$$\rho_F(S) = \|\boldsymbol{\tau}^0 + \mathbf{f} - \boldsymbol{\pi}S\| - \boldsymbol{\pi}^T(\boldsymbol{\tau}^0 + \mathbf{f} - \boldsymbol{\pi}S). \tag{21}$$

An extended formula accounting for more point forces along the cable and thermal loads is available in Impollonia et al. (2011).

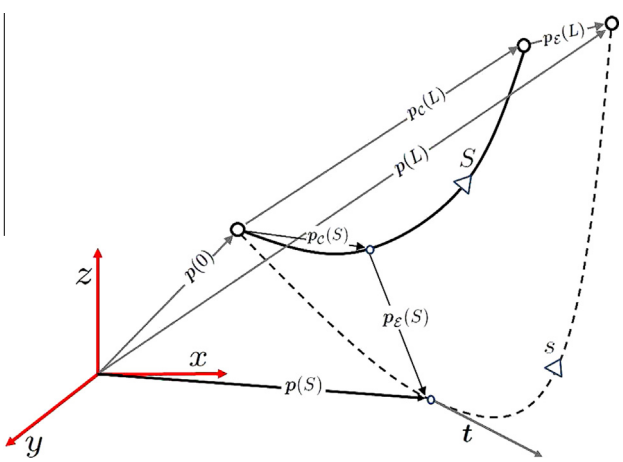

Fig. 2. Unstrained configuration (solid) with $0 \leqslant S \leqslant L$ and strained configuration (dashed) with $0 \leqslant s \leqslant l$ under uniformly distributed load.

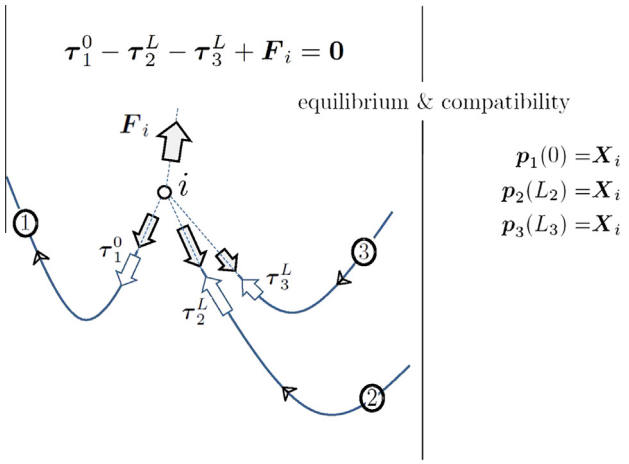

Fig. 3. Equilibrium at node *i* and compatibility for cables connected to node *i*. Gray arrows are the forces acting on the node.

3. Nodal equilibrium and compatibility conditions for cable structures

The problem equations for cable nets are now defined. These are: (*i*) equilibrium equations at free nodes and (*ii*) compatibility equations, which are expressed as connectivity conditions at the end node of each cable exploiting Eq. (16) or (20).

Assume that the cable net has $N = N_1 + N_2$ nodes, with N_1 free nodes and N_2 fixed nodes, and M cables. For the sake of simplicity free nodes will be consecutively numbered from 1 to N_1 whereas the fixed nodes from $N_1 + 1$ to N. Let i be the generic free node of the net, with $i = 1, 2, \dots N_1$, and j the generic cable connected to the node j_1 (origin of the cable) and j_2 (end of the cable), with $j = 1, 2, \dots M$ and $j_1, j_2 = 1, 2 \dots N$. The equilibrium of the ith node, joining n_i cables, is given by

$$\left(\sum_j^{n_i} \boldsymbol{\tau}_j^*\right) + \mathbf{F}_i = \mathbf{0}, \quad (i = 1, 2, \dots N_1) \tag{22}$$

where $\mathbf{F}_i$ is the external force applied to the node and $\boldsymbol{\tau}_j^*$, if only distributed load is present, is given by

$$\boldsymbol{\tau}_j^* = \begin{cases} +\boldsymbol{\tau}_j^0, & \text{if } j_1 = i, \text{ (i.e. } \textit{the cable origin is at the node}) \\ -\boldsymbol{\tau}_j^L = -\left(\boldsymbol{\tau}_j^0 - \mathbf{q}_j L_j\right), & \text{if } j_2 = i, \text{ (i.e. } \textit{the cable end is at the node}) \end{cases} \tag{23}$$

According to the connectivity of the net, the jth cable is joined to nodes j_1 (cable origin) and j_2 (cable end), so that the compatibility equations relevant to the jth cable under uniform distributed load are

$$\mathbf{p}_j(0) = \mathbf{X}_{j_1}, \quad \mathbf{p}_j(L_j) = \mathbf{X}_{j_2}, \tag{24}$$

being $\mathbf{X}_{j_1}$ and $\mathbf{X}_{j_2}$ the coordinates of the nodes of the net (free or fixed) in the strained configuration. The position of the cable ends is derived from Eq. (16) and is given by

$$\begin{aligned} \mathbf{p}_j(L_j) = {} & \frac{q_j L_j}{E_j A_j}\left(\frac{\boldsymbol{\tau}_j^0}{q_j} - \boldsymbol{\pi}_j \frac{L_j}{2}\right) + \left(\mathbf{I} - \boldsymbol{\pi}_j \boldsymbol{\pi}_j^T\right)\frac{\boldsymbol{\tau}_j^0}{q_j} \ln\left[\frac{\rho_j(L_j)}{\rho_j(0)}\right] \\ & - \boldsymbol{\pi}_j \left(\left\|\frac{\boldsymbol{\tau}_j^0}{q_j} - \boldsymbol{\pi}_j L_j\right\| - \left\|\frac{\boldsymbol{\tau}_j^0}{q_j}\right\|\right) + \mathbf{p}_j(0), \quad (j = 1, 2 \dots M). \end{aligned} \tag{25}$$

Analogous equations can be written if a point force is acting on the cable referring to Eqs. (19) and (20). An example of equilibrium and compatibility relationships is shown in Fig. 3.

Assume that unstrained length L_j, cross sectional area A_j, elastic modulus E_j and load $\mathbf{q}_j$ be assigned for each cable and nodal forces $\mathbf{F}_i$ be given for each free node. Then, the $3N_1$ equilibrium equations (22) and the $3M$ compatibility conditions (25) realize a non linear set of equations with unknowns given by $3N_1$ coordinates of free nodes, $\mathbf{X}_i = \{X_i, Y_i, Z_i\}$, and $3M$ components of cable tension at cables origin, $\boldsymbol{\tau}_j^0 = \{\tau_{j,x}^0, \tau_{j,y}^0, \tau_{j,z}^0\}$.

The system of equations allows the structural analysis of three dimensional cable nets under external nodal forces, uniform distributed loads and point forces however oriented on the cables. On the other hand it is not well suited for the initial design, i.e. the form-finding of the net, as the initial cable lengths must be imposed. The latter problem is tackled in the following according to a strategy proposed in Cuomo and Greco (2012).

4. Form-finding

The form-finding strategy, named catenary force densities methods, C-FDM, is resorted to. The strategy is based on the force density method for slack cable nets and accounts for self weight in the form-finding.

The procedure is clearly non-linear because the length of the cables are unknown so as their total weights. For this reason we first consider a linear step, i.e. the classical form-finding problem neglecting self weight, by linear force density method (L-FDM). The solution of the linear step is the initializing solution for the successive non linear C-FDM. A uniform vertical conservative loads acting on the cable, $\mathbf{q} = q_z \boldsymbol{\pi}_z$, ia assumed for each cable ($\boldsymbol{\pi}_z = \{0, 0, -1\}$) as self-weight. The equilibrium equations of the ith node are

$$\begin{aligned} \sum_j^{n_i} \boldsymbol{\tau}_{j,x}^* &= 0, \\ \sum_j^{n_i} \boldsymbol{\tau}_{j,y}^* &= 0, \\ \sum_j^{n_i} \boldsymbol{\tau}_{j,z}^* &= 0. \end{aligned} \tag{26}$$

The following decomposition for the tensile force at cable origin is considered

$$\boldsymbol{\tau}_j^0 = \mathbf{V}_j^0 + \mathbf{H}_j^0, \tag{27}$$

where $\mathbf{V}_j^0$ and $\mathbf{H}_j^0$ are vertical and horizontal vectors, respectively, given by

$$\mathbf{V}_j^0 = \left(\boldsymbol{\pi}_z \boldsymbol{\pi}_z^T\right)\boldsymbol{\tau}_j^0, \quad \mathbf{H}_j^0 = \left(\mathbf{I} - \boldsymbol{\pi}_z \boldsymbol{\pi}_z^T\right)\boldsymbol{\tau}_j^0. \tag{28}$$

The horizontal components are

$$\begin{aligned} \tau_{j,x}^0 = \tau_{j,x}^L = H_{j,x}^0 = \|\mathbf{H}_j^0\| \frac{X_{j_2} - X_{j_1}}{\Delta h_j}, \\ \tau_{j,y}^0 = \tau_{j,y}^L = H_{j,y}^0 = \|\mathbf{H}_j^0\| \frac{Y_{j_2} - Y_{j_1}}{\Delta h_j}, \end{aligned} \tag{29}$$

where $\Delta h_j = \sqrt{(X_{j_2} - X_{j_1})^2 + (Y_{j_2} - Y_{j_1})^2}$ is the horizontal span between cable extremities. The vertical components of the tensile stress at the cable ends according to the catenary solution, see Cuomo and Greco (2012), are given by

$$V_j^0 = \frac{\|\mathbf{H}_j^0\|}{\Delta h_j}\eta_j \frac{\mathrm{Cosh}[\eta_j]}{\mathrm{Sinh}[\eta_j]}(Z_{j_2} - Z_{j_1}) - \frac{q_{z,j}L_j}{2},$$
$$V_j^L = \frac{\|\mathbf{H}_j^0\|}{\Delta h_j}\eta_j \frac{\mathrm{Cosh}[\eta_j]}{\mathrm{Sinh}[\eta_j]}(Z_{j_2} - Z_{j_1}) + \frac{q_{z,j}L_j}{2}, \tag{30}$$

with

$$\eta_j = \frac{q_{z,j}\Delta h_j}{2\|\mathbf{H}_j^0\|}. \tag{31}$$

By introducing the cable force density

$$Q_j = \frac{\|\mathbf{H}_j^0\|}{\Delta h_j}, \tag{32}$$

the nodal equilibrium reduces to

$$\sum_j^{n_i} \pm Q_j(X_{j_2} - X_{j_1}) = 0,$$
$$\sum_j^{n_i} \pm Q_j(Y_{j_2} - Y_{j_1}) = 0, \tag{33}$$
$$\sum_j^{n_i} \frac{q_{z,j}}{2}\left(\pm\frac{\mathrm{Cosh}[\eta_j]}{\mathrm{Sinh}[\eta_j]}(Z_{j_2} - Z_{j_1}) - L_j\right) = 0,$$

where the sign $(+)$ must be imposed if $j_1 = i$ (i.e. the node is the origin of the jth cable), whereas the sign $(-)$ should be retained if $j_2 = i$ (i.e. the node is the end of the jth cable).

The unstrained length of the jth cable is given by

$$L_j = l_j - \Delta L_{e,j}, \tag{34}$$

where the length of the strained cable is

$$l_j = \sqrt{\frac{l_j^2}{\eta_j^2}\mathrm{Sinh}[\eta_j] + (Z_{j_2} - Z_{j_1})^2} \tag{35}$$

and the elastic increment $(\Delta L_{e,j})$ is given by

$$\Delta L_{e,j}(\|\mathbf{H}_j^0\|, V_j^0, L_j) = \frac{\mu(V_j^0) - \mu(V_j^L)}{2EAq_{z,j}}. \tag{36}$$

The operator $\mu(\bullet)$ is given by

$$\mu(\bullet) = (\bullet)\sqrt{(\bullet)^2 + \|\mathbf{H}_j^0\|^2} + \|\mathbf{H}_j^0\|^2 \mathrm{ArcSinh}\left(\frac{(\bullet)}{\|\mathbf{H}_j^0\|}\right). \tag{37}$$

By substituting Eq. (34) into (33) a non linear set of equations with unknown $\{X_i, Y_i, Z_i\}$ is obtained when the force density is assigned at each cable.

The solution of the form-finding neglecting self weight, according to L-FDM, i.e. the solution of the following linear system

$$\sum_j^{n_i} \pm Q_j(X_{j_2} - X_{j_1}) = 0,$$
$$\sum_j^{n_i} \pm Q_j(Y_{j_2} - Y_{j_1}) = 0, \tag{38}$$
$$\sum_j^{n_i} \pm Q_j(Z_{j_2} - Z_{j_1}) = 0,$$

is adopted as the initial step for the solution of the non linear equilibrium equations (33).

5. Numerical examples

The capabilities of the proposed procedure are preliminarily assessed by examining a simple slack cable net, first designed by the proposed C-FDM and successively loaded with a nodal force and a point force along a cable. Finally, the procedure is applied to the form-finding and successive structural analysis of a net in presence of struts. Namely, the plane Jawerth cable structure (Mollmann, 1970) is analyzed along with its spatial version, where the effectiveness of the proposed strategy is fully exploited.

5.1. A 5-cable net

The simple very slack 5-cable net reported in Fig. 4(a) is considered. A form-finding by means of C-FDM is first performed, then starting from the obtained configuration two load cases are applied: a nodal force and one point force on a cable.

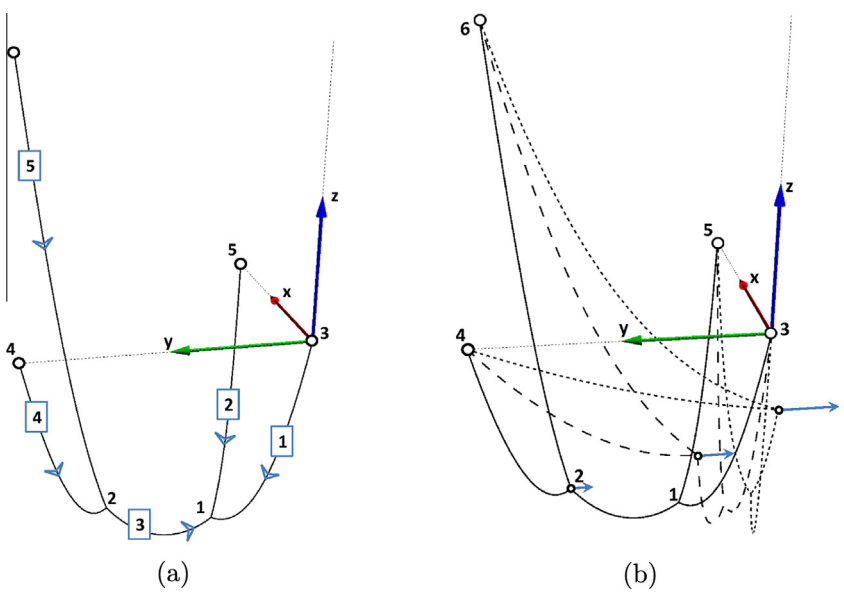

Fig. 4. Initial configuration, topology and labels of nodes and cables of the cable net (a); different configurations at the load $F_y = 0, -3, -10$ [daN], respectively plotted with continuous, dashed and pointed line (b).

Table 1
Node positions.

Node	Unelastic			Elastic		
	x [m]	y [m]	z [m]	x [m]	y [m]	z [m]
$\mathbf{P}_1$	0.5	0.25	−1.1143	0.4999	0.2499	−1.1148
$\mathbf{P}_2$	0.5	0.75	−0.9954	0.4994	0.7500	−0.9963
$\mathbf{P}_3$	0	0	0	0	0	0
$\mathbf{P}_4$	1	0	0	1	0	0
$\mathbf{P}_5$	0	1	0	0	1	0
$\mathbf{P}_6$	1	1	1	1	1	1

Table 2
Unelastic case ($EA = \infty$).

	L_j [m]	$\|\mathbf{H}_j^0\|$ [daN]	V_j^0 [daN]	V_j^L [daN]
Cable-1	1.2887	0.5870	−2.7928	−0.2153
Cable-2	1.2887	0.5870	−2.7928	−0.2153
Cable-3	0.5912	0.5250	−0.7517	0.4307
Cable-4	1.1874	0.5870	−2.5310	−0.1561
Cable-5	2.0978	0.5870	−4.7911	−0.5955

Table 3
Elastic case ($EA = 5000$ [daN]).

	ΔL_j [m]	$\|\mathbf{H}_j^0\|$ [daN]	V_j^0 [daN]	V_j^L [daN]
Cable-1	0.000424	0.5864	−2.7928	−0.2153
Cable-2	0.000424	0.5870	−2.7934	−0.2160
Cable-3	0.000075	0.5247	−0.7511	0.4313
Cable-4	0.000357	0.5870	−2.5328	−0.1580
Cable-5	0.001163	0.5861	−4.7887	−0.5931

5.1.1. Form-finding

The initial design is generated considering a self weight $q_z = 2.0$ [daN/m] and force densities $Q_j = 1.05$ [daN/m] for each cable. The axial stiffness of each cable is set to $EA = 5000$ [daN]. Also the unelastic case ($EA = \infty$) is treated.

Table 1 shows the nodal coordinates of free nodes ($\mathbf{P}_1, \mathbf{P}_2$) and fixed nodes ($\mathbf{P}_3, \mathbf{P}_4, \mathbf{P}_5$ and $\mathbf{P}_6$). Table 2 and Table 3 list vertical and horizontal components of tensile forces, obtained by means of C-FDM, for the unelastic and elastic case, respectively. The unstrained length L_j, which is non affected by cable elasticity, is reported in Table 2, whereas cable elongation ΔL_i is show in Table 3.

As expected, due to cable slackness, elasticity plays a minor role and the horizontal component of the tensile force, $\|\mathbf{H}_j^0\|$, is smaller when elasticity is accounted for.

5.1.2. Analysis under increasing nodal force

An horizontal force is applied to node 2 of the elastic net. The force is directed in the y-direction and is incremented from $F_y = 0$, to $F_y = -10$ [daN]. Fig. 4(b) plots the configurations due to the values of nodal force $F_y = 0, -3, -10$ [daN].

The horizontal and vertical components of the axial force at the first end of each cable are plotted in Fig. 5(a). The results evidence the transition in the behavior of cable 4 from the initial slack catenary to the final linear elastic truss-like solution. Cable 4 attains a straight configuration when the force is increased, whereas the other cables maintain a slack configuration and their elastic strain is only slightly influenced by the nodal force increment. The horizontal force H^0 on cable 1 reduces to zero, meaning that this cable has become completely slack and transmits the vertical weight only to end nodes. Fig. 5(b) plots the displacements of the two free nodes, and reveals a strong non-linear behavior.

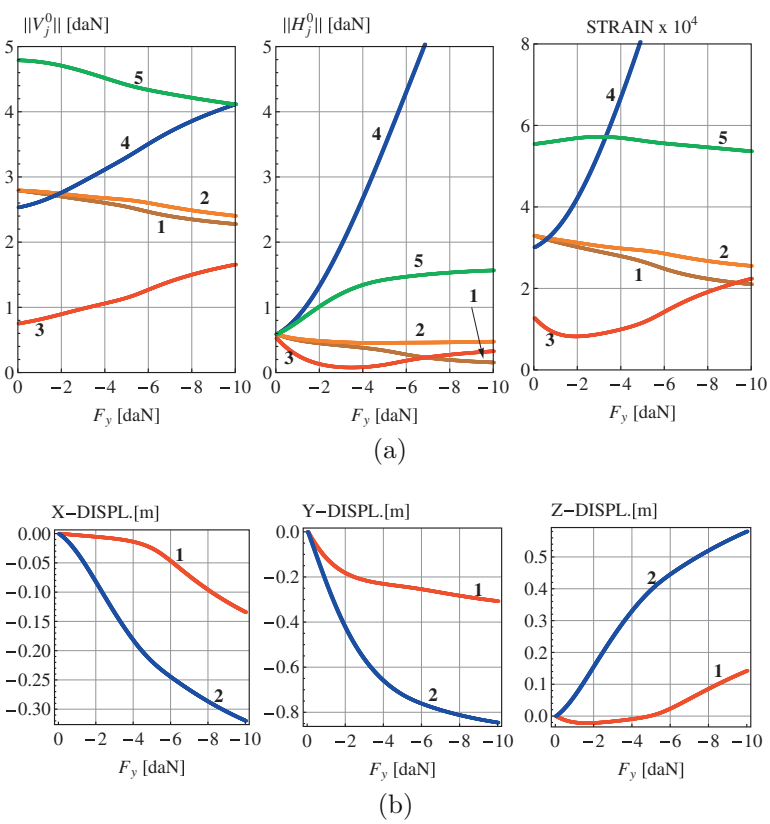

Fig. 5. Incremental evolutions of $\|\mathbf{V}_j^0\|, \|\mathbf{H}_j^0\|$ and elastic elongation for each cable (a); displacement components of the two free nodes, P_1 and P_2 (b).

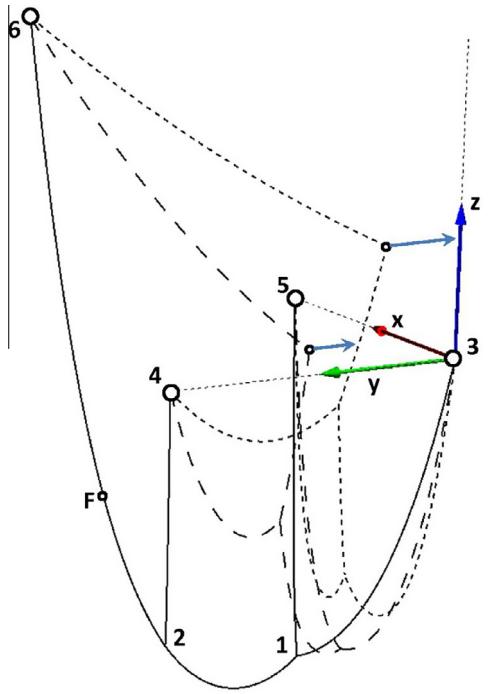

Fig. 6. Different configurations obtained for $q_z = 2$ [daN] on all cables and $F_y = 0, -6, -10$ [daN], respectively plotted with continuous, dashed and pointed line (b).

In particular the stiffening effects due to cable 4 is evident from the y-displacement plot.

5.1.3. One point force along the cable

The same force of the previous analysis is now applied to abscissa $S_5 = 0.84\,[m]$ of cable 5, (cable origin is at node 6).

Fig. 6 depicts the configurations related to three values of intensity of the point force ($F_y = 0, -6, -10$ [daN]). Cable 5 is modelled by the element defined in Section 2.2.2. Fig. 7(a) displays the incremental evolution for vertical and horizontal components of the axial force at the origin of the cables and their elastic elongation. Fig. 7(b) plots the displacements of free nodes and of the loaded point of cable 5. A linear trend in the incremental behavior of the cable 5 appears when the force increases.

The numerical application assesses a god performance of the element to capture the different behaviors in the slack and in the truss-like regime.

5.2. Plane cable roof

The symmetric roof truss, shown in Fig. 8, designed by Jawerth for the Johanneshov Ice Stadium in Stockholm, is considered with cable sections reported in Table 4. This structure has already been studied by Mollmann (1970) and successively by Ahmadi-Kashani and Bell (1988a).

The initial pre-stress distribution and the initial geometry are defined in Mollmann (1970). Accordingly, the force densities

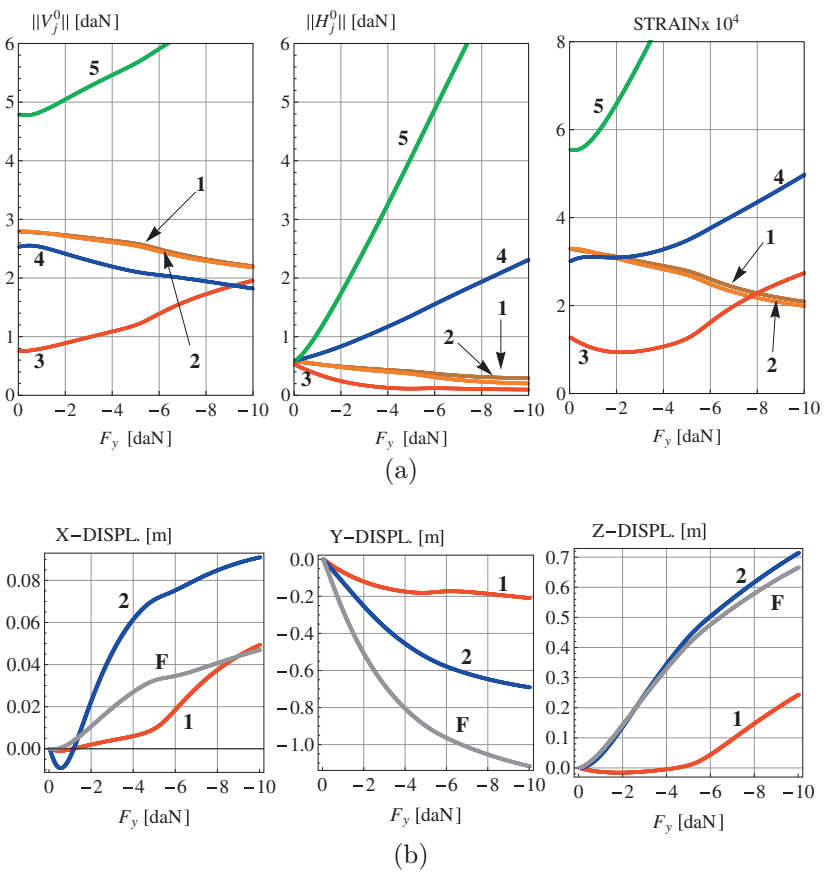

Fig. 7. Incremental evolution of $\|\mathbf{V}_j^0\|, \|\mathbf{H}_j^0\|$ and elastic elongation for each cable (a); displacement components of the two free nodes, P_1 and P_2, and of the loaded point of cable 5 marked with F (b).

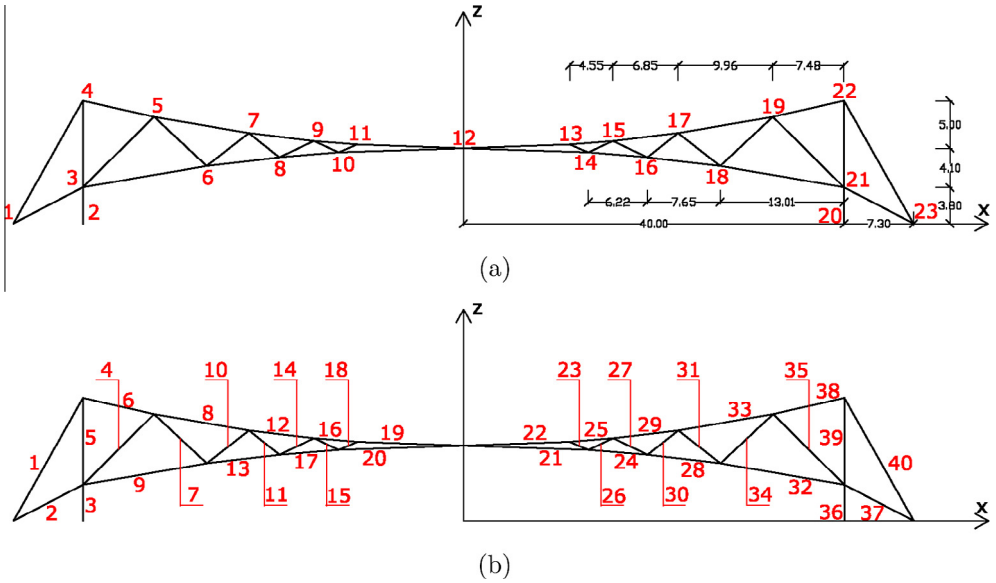

Fig. 8. Geometry of the *Jawerth* cable truss with node labels (a) and cable labels (b).

Table 4
Cross sections.

Element group	Area [cm^2]
Top cable	25.1
Bottom cable	17.2
Diagonals	2.84
Longer stays	63.7
Shorter stays	15.9
Columns	222.6

Table 5
Force density Q_j.

Top [kN/m]	Bottom [kN/m]	Diagonal [kN/m]
$Q_6 = 68.397$	$Q_9 = 42.217$	$Q_4 = 2.110$
$Q_8 = 51.695$	$Q_{13} = 70.291$	$Q_7 = 2.261$
$Q_{12} = 77.494$	$Q_{17} = 82.825$	$Q_{10} = 5.422$
$Q_{16} = 122.404$	$Q_{20} = 35.065$	$Q_{11} = 2.507$
$Q_{19} = 55.249$		$Q_{14} = 8.436$
		$Q_{15} = 1.748$
		$Q_{18} = 30.431$

$Q_j = \|\mathbf{H}_j^0\|/\Delta h_j$ have been evaluated for top, bottom and diagonal cables and reported in Table 5. The modulus of elasticity $E = 14790\,[\text{kN/cm}^2]$ is assumed for all the elements (including columns). As in Ahmadi-Kashani and Bell (1988a), element self weight is determined assuming a density $\rho = 77.784\,[\text{kN/m}^3]$.

The unstrained lengths of stays (element n. 1, 2, 37, 40) and columns (element n. 3, 5, 36, 39) are determined imposing the coordinates of their end nodes (see Fig. 8), and equilibrium at nodes 3, 4 and 21, 22. The unstrained length for the elements is listed in Table 6.

First we compare our results with those obtained by Mollmann (1970) and successively by Ahmadi-Kashani and Bell (1988a), referred to a dead load of the roof equal to 1.786 [kN/m] and applied to top cable. The unstrained lengths are those given in Table 6. Table 7 shows the results obtained by Mollmann (1970) and Ahmadi-Kashani and Bell (1988a) and the proposed strategy for the considered load case. As appears from Table 7 there are no significative differences in the results obtained for top, bottom and stay cables (i.e. taut elements).

Table 6
Unstrained length L_j.

Top [m]	Bottom [m]	Diagonal [m]	Columns [m]	Stays [m]
$L_6 = 7.692$	$L_9 = 13.142$	$L_4 = 10.510$	$L_3 = 3.799$	$L_1 = 14.807$
$L_8 = 10.124$	$L_{13} = 7.742$	$L_7 = 7.558$	$L_5 = 9.098$	$L_2 = 8.201$
$L_{12} = 6.863$	$L_{17} = 6.265$	$L_{10} = 5.743$		
$L_{16} = 4.555$	$L_{20} = 13.169$	$L_{11} = 4.068$		
$L_{19} = 11.163$		$L_{14} = 4.090$		
		$L_{15} = 2.815$		
		$L_{18} = 2.168$		

Table 7
Element forces under dead load.

el. group	n.	Mollmann (1970) [tons]	Ahmadi-Kashani and Bell (1988a) [tons]	Present analysis [tons]
Columns	3	−151.9	−154.63	−153.47
	5	−137.9	−139.40	−138.03
Stays	1	140.5	140.00	141.06
	2	46.4	46.97	47.34
Top-c.	6	70.9	70.71	71.16
	8	69.6	69.22	68.37
	12	69.1	68.70	69.54
	16	68.9	68.48	69.36
	19	72.3	72.15	73.15
Bottom-c.	9	41.5	41.55	41.75
	13	41.4	41.50	41.36
	17	41.1	41.19	40.95
	20	38.6	38.54	37.89
Diagonals	4	1.00	1.00	1.40
	7	1.80	2.00	1.38
	10	1.40	1.50	0.97
	11	1.40	1.51	1.10
	14	1.40	1.50	1.11
	15	1.40	1.47	2.65
	18	3.90	4.18	5.21

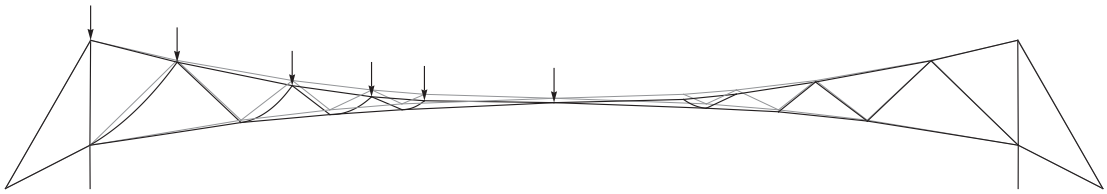

Fig. 9. Initial ($F = 0$) and final ($F = 57.8$ [kN]) configurations of the net.

Let us now consider the load case defined by vertical forces applied to the nodes of half top cable with intensity F. In order to show the performance of the numerical procedure, the intensity of the force is increased from $F = 0$ to $F = 57.8$ [kN]. The initial and final configurations of the cable-net are shown in Fig. 9. The unloading of diagonals, especially those under vertical nodal forces, is evident.

The ratio $\|\boldsymbol{\tau}^0\|/\|\boldsymbol{\tau}^0_{pre-stress}\|$, where $\boldsymbol{\tau}^0$ is the tensile force in the loaded configuration and $\boldsymbol{\tau}^0_{pre-stress}$ is the same quantity for $F = 0$, are reported in Figs. 10 and 11. As expected, the tensile force of the top cable increases with the load; an higher increment is shown for the loaded side of the net (left side), see Fig. 10(a). On the other hand, the bottom cable shows a reduction of the tensile force when the load increases, see Fig. 10(b).

A more complex scenario appears for the diagonals. Some of them become slack (elements n. 4, 10, 14, 18, 23 and 27) when the force increases, see Fig. 11(a). Diagonals n. 11 and 15 exhibit

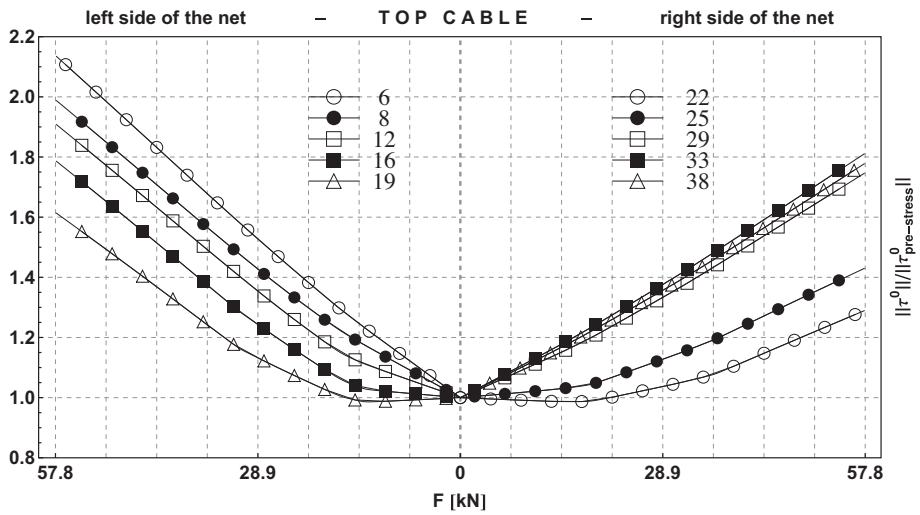

(a)

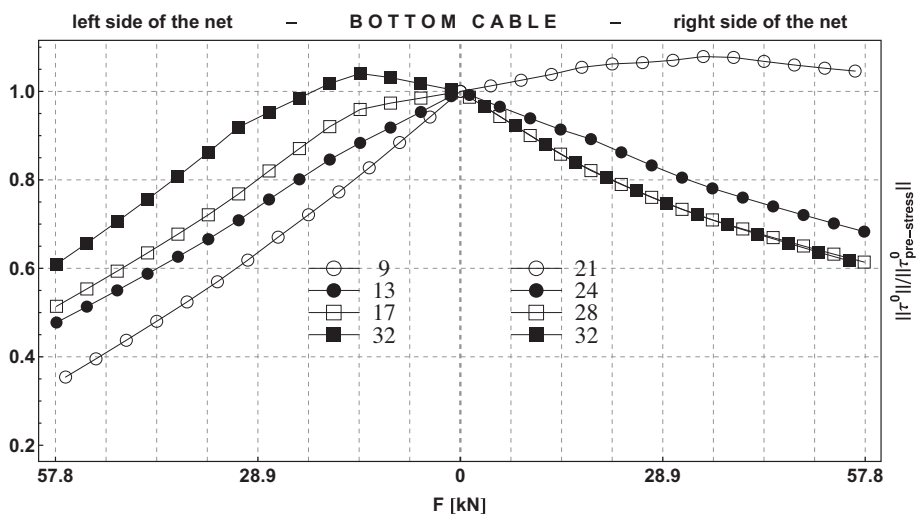

(b)

Fig. 10. Results of the incremental analysis for top cables (a) and bottom cables (b).

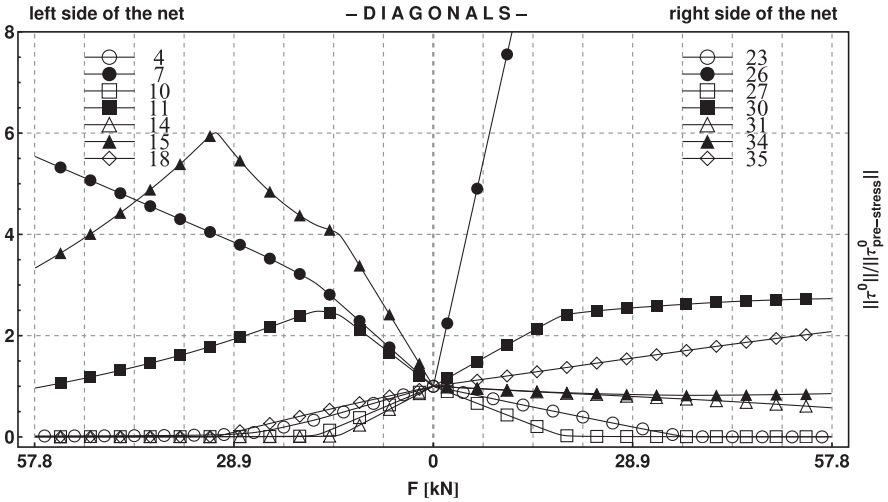

(a)

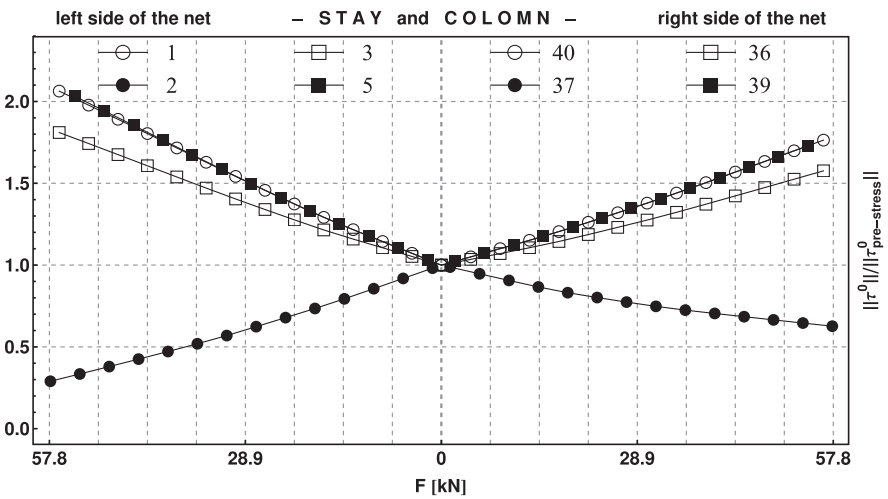

(b)

Fig. 11. Results of the incremental analysis for diagonal cables (a) and stay cables and columns (b).

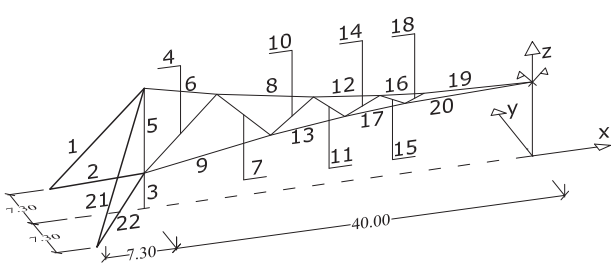

Fig. 12. Labels of half 3D cable roof.

a non monotonous trend for increasing forces; high sensitivity of the tensile force at diagonal n. 26 is evident. It can be observed that diagonal cables are most affected by node force increments when compared with other cables.

Finally, Fig. 11(b) shows that shorter stay cables (element n. 2 and 37) lose tension when nodal forces increases, whereas an opposite trend is shown by longer stay cables. The axial compressive force increment on columns is basically linearly related to nodal force intensity.

5.3. Space cable roof

The structure of the previous section is investigated for a different configuration of the stay cables. These are now positioned out of the main vertical plane (the plane containing all free nodes), as shown in Fig. 12, where half of the symmetric three-dimensional cable roof is depicted. The net is now capable to withstand horizontal actions along y-direction. The longer stays have unstrained length $L_1 = L_{21} = 16.50\,[\mathrm{m}]$; for the shorter ones $L_2 = L_{22} = 10.96\,[\mathrm{m}]$. The other elements of the structure are defined as in the previous section, since the same force densities are adopted (see Table 5 and first four columns of Table 6).

A structural analysis is conducted under an incremental horizontal load (orthogonal to the main vertical plane) uniform on each element of the net (cables and columns) and defined as $q_j = \lambda * q_{ref} * \phi_j$, where ϕ_j is the diameter of the element, $q_{ref} = 2.6\,[\mathrm{kN/m}]$ and the load factor $\lambda \in [0, 1]$. The load condition could be a rough model of wind action on the net. The columns

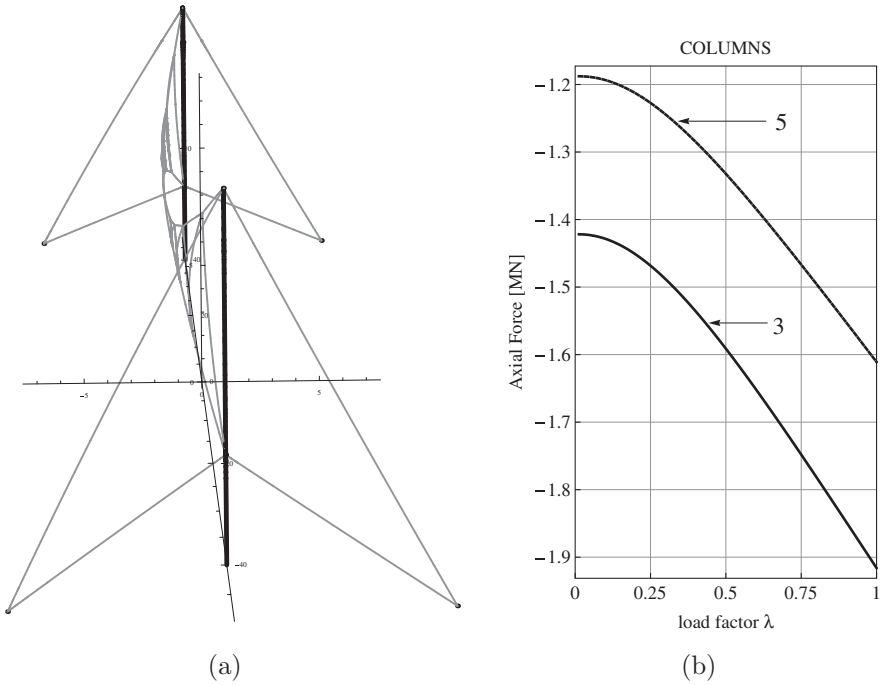

Fig. 13. Results of the incremental analysis: final configuration of the net (a) and compressive axial force on the columns (b).

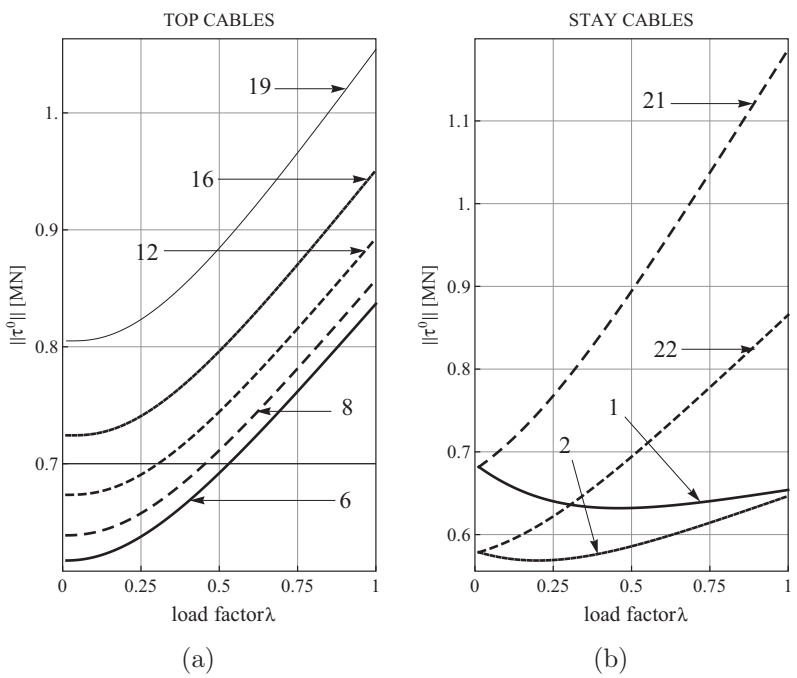

Fig. 14. Results of the incremental analysis: tensile force at the first end for top (a) and stay cables (b).

have hollow circular cross section with diameter $\phi = 0.5$ [m], whereas all the cables have solid circular section and their diameter can deduced by Table 4.

The results of the incremental analysis are reported in Figs. 13–16 and the final configuration ($\lambda = 1$) is depicted in Fig. 13(a).

The onset of the out-plane load is balanced by up-wind stays as only the tension of cables 21 and 22 exhibit a prompt increment, whereas down-wind stays are initially unloaded (see Fig. 14(b)). All the other elements do not vary appreciably their tension when the load factor is small. In fact as depicted in Figs. 13(b), 14(a), 15(a) and 15(b) an horizontal tangent appears for $\lambda \to 0$. When λ increases the stiffness gain is evident and tensile stress rises in all elements but in the longer down-wind stay (element n.1). The geometric stiffening behavior is evident from the trend of y-displacement of the center of the net plotted in Fig. 16.

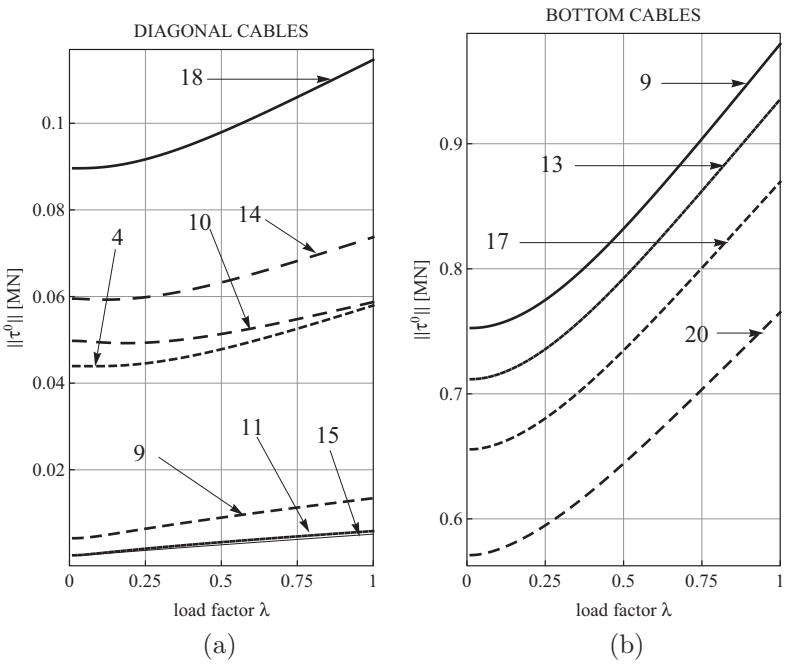

Fig. 15. Results of the incremental analysis: tensile force at the first end of the diagonal (a) and bottom cables (b).

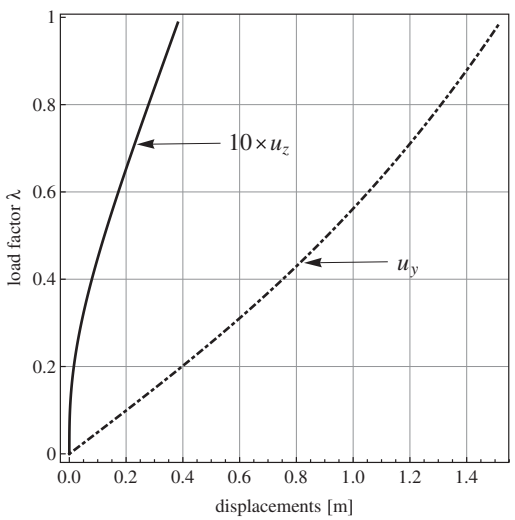

Fig. 16. Displacement at the center of the net versus load factor.

6. Conclusions

A general procedure has been developed which can accurately solve cable structures under different load conditions. The procedure relies on the three dimensional vector form solution of the catenary equation which allows a straight derivation of compatibility conditions in the global reference system. Both the case of uniformly distributed load and point force generally oriented in space can be handled. The non-linear algebraic governing equations with unknowns given by cable tension components and free node coordinates are easily assembled according to cable connectivity and position of fixed nodes. The numerical solution may be conveniently pursued by the Newton–Raphson method by choosing suitable initial conditions under cable pre-stress and self weight. To this aim the catenary force density method is resorted to in order to determine the initial cable stresses and configuration of the net. The effectiveness of the method is shown for slack cable nets, the plane Jawerth cable net and its three dimensional version.

References

Ahmadi-Kashani, K., Bell, A.J., 1986. The representation of cables subjected to general loading. Int. J. Space Struct. 2, 29–44.

Ahmadi-Kashani, K., Bell, A.J., 1988a. The analysis of cables subject to uniformly distributed loads. Eng. Struct. 10 (3), 174–184.

Ahmadi-Kashani, K., Bell, A.J., 1988b. Representation of cables in space subjected to uniformly distributed loads. Int. J. Space Struct. 3 (4), 221–230.

Andreu, A., Gil, L., Roca, P., 2006. A new deformable catenary element for the analysis of cable net structures. Comput. Struct. 84 (29–30), 1882–1890.

Argyris, J.H., Angelopoulos, T., Bichat, B., 1974. A general method for shape finding of lightweight tension structures. Comput. Methods Appl. Mech. Eng. 30, 263–284.

Bletzinger, K.U., Ramm, E., 1999. A general finite element approach to the form finding of tensile structures by the updated reference strategy. Int. J. Space Struct. 14 (2), 131–146.

Bruno, D., Leonardi, A., 1999. A nonlinear structural models in cableway transport system. Simul. Pract. Theor. 7 (3), 207–218.

Cuomo, M., Greco, L., 2012. On the force density method for slack cable nets. Int. J. solids Struct. 49 (13), 1526–1540.

Deng, H., Jiang, Q., Kwan, A., 2005. Shape finding of incomplete cable-strut assemblies containing slack and prestressed elements. Comput. Struct. 83, 1767–1779.

Di Paola, M., 1998. Non-linear dynamic analysis of cable-suspended structures subjected to wind actions. J. Wind Eng. Ind. Aerodyn. 74–79, 91–109.

Freire, A.M.S., Negrão, J.H.O., Lopes, A.V., 2006. Geometrical nonlinearities on the static analysis of highly flexible cable-stayed bridges. Comput. Struct. 84, 2128–2140.

Haber, R., Abel, J., 1982. Initial equilibrium solution methods for cable reinforced membranes part ii-implementation. Comput. Methods Appl. Mech. Eng. 30, 285–306.

Impollonia, N., Ricciardi, G., Saitta, F., 2011. Static of elastic cables under 3d point forces. Int. J. Solid Struct. 48, 1268–1276.

Impollonia, N., Ricciardi, G., Saitta, F., 2011a. Vibrations of inclined cables under skew wind. Int. J. Non-Linear Mech. 46 (7), 907–919.

Impollonia, N., Ricciardi, G., Saitta, F., 2011b. Dynamics of shallow cables under turbulent wind: a nonlinear finite element approach. Int. J. Struct. Stab. Dyn. 11 (4), 755–774.

Irvine, H.M., 1992. Cable Structures. Dover Publications, New York.

Jayaraman, H.B., Knudson, W.C., 1981. A curved element for the analysis of cable structures. Comput. Struct. 14 (3–4), 325–333.

Lazzari, M., Saetta, A., Vitaliani, R., 2001. Non-linear dynamic analysis of cable-suspended structures subjected to wind actions. Comput. Struct. 79 (9), 953–969.

Lee, C.L., Perkins, N.C., 1992. Oscillations of suspended cables containing a two-to-one internal resonance. Nonlinear Dyn. 3, 465–490.
Lepidi, M., Gattulli, V., Vestroni, F., 2007. Static and dynamic response of elastic suspended cables with damage. Int. J. Solid Struct. 44 (25–26), 8194–8212.
Luongo, A., Piccardo, G., 1998. Non-linear galloping of sagged cables in 1:2 internal resonance. J. Sound Vib. 214 (5), 915–936.
Luongo, A., Piccardo, G., 2008. A continuous approach to the aeroelastic stability of suspended cables in 1:2 internal resonance. J. Vib. Control 14 (1–2), 135–157.
Mollmann, H., 1970. Analysis of plane prestressed cable structures. J. Struct. Div. ASCE 96 (ST10), 2059–2082.
Pauletti, R., Pimenta, P., 2008. The natural force density method for the shape finding of taut structures. Comput. Methods Appl. Mech. Eng. 197, 4419–4428.
Peyrot, A.H., Goulois, A.M., 1978. Analysis of flexible transmission lines. J. Struct. Div. ASCE 104 (ST5), 763–779.
Peyrot, A.H., Goulois, A.M., 1979. Analysis of cable structures. Comput. Struct. 10 (5), 805–813.
Sagatun, S., 2001. The elastic cable under the action of concentrated and distributed forces. J. Offshore Mech. Arct. Eng. 123 (1), 43–45.
Schek, H.J., 1974. The force density method for form finding and computation of general networks. Comput. Methods Appl. Mech. Eng. 3, 115–134.
Such, M., Jimenez-Octavio, J., Carnicero, A., Lopez-Garcia, O., 2009. An approach based on the catenary equation to deal with static analysis of three dimensional cable structures. Eng. Struct. 31 (9), 2162–2170.
Thai, H.T., Kim, S.E., 2011. Nonlinear static and dynamic analysis of cable structures. Finite Elem. Anal. Des. 47 (3), 237–246.